ELSEVIER

Polymer 40 (1999) 2619–2624

polymer

Thermal micro ATR/FT-IR spectroscopic system for quantitative study of the molecular structure of poly(*N*-isopropylacrylamide) in water

Shan-Yang Lin[a,*], Ko-Shao Chen[b], Liang Run-Chu[b]

[a]*Department of Medical Research and Education, Veterans General Hospital—Taipei, Taipei, Taiwan, ROC*
[b]*Tatung Institute of Technology, Taipei, Taiwan, ROC*

Received 6 May 1998; revised 12 June 1998; accepted 29 June 1998

Abstract

The molecular interactions in poly (*N*-isopropylacrylamide) (PNIPAAM) aqueous solution have been quantitatively investigated by using a newly developed thermal micro attenuated total reflection/Fourier transform infrared (ATR/FT-IR) spectroscopic system. PNIPAAM was prepared by the w/o emulsion method and its lower critical solution temperature (LCST) was examined by cloud point measurement and differential scanning calorimetry. The LCST of this PNIPAAM in water was about 33°C, which was also confirmed by this thermal micro ATR/FT-IR spectroscopic system. Using this novel spectroscopic system with curve-fitting program, we found that below the LCST the molecular structure of PNIPAAM in water exhibited a predominantly intermolecular hydrogen bonding (about 50%–70% of total molecular interaction estimated from amide I band) between PNIPAAM and water. However, above LCST the intramolecular hydrogen bonded conformation was about 70% in total molecular interaction (estimated from amide II band). Moreover, the hydrophobic interaction of methyl group in PNIPAAM molecule increased 1.5 times when the temperature was above the LCST. The results quantitatively indicate that the intermolecular interactions might occur mainly between PNIPAAM molecules and water when temperature was below the LCST. When the temperature was above the LCST, however, PNIPAAM molecules in water were aggregated due to both the intramolecular interactions within PNIPAAM molecules and the hydrophobic interactions in system.

Keywords: Poly(*N*-isopropylacrylamide); LCST; Thermal micro ATR/FT-IR

1. Introduction

Recently, poly (*N*-isopropylacrylamide) (PNIPAAM) as an intelligent polymer has received growing interest in drug delivery systems and in biotechnology [1–6], due to its thermal-responsive function. PNIPAAM has not only hydrophilic groups (NH, C=O) but also a hydrophobic group (isopropyl), thus the hydrophilic interaction as well as hydrophobic interaction may play a dominant role in the thermo-shrinking transition [7]. It is well known that PNIPAAM is insoluble in water above the lower critical solution temperature (LCST), about 32°–33°C [7,8], and is reversibly solubilized below that temperature when PNIPAAM exists as flexible but extended coils in aqueous solution. Above the LCST, it shrinks as aggregates. The driving force for this coil-to-globule transition is associated with the temperature-dependent molecular interactions, mainly hydrogen bonding and hydrophobic interaction [7,9,10]. However, there has been much debate as to whether hydrophobic effect or hydrogen bonding effect is a dominant driving force in PNIPAAM aqueous solution below and above LCST. Moreover, how much quantitative contribution that both effects can afford to molecular interactions is hardly studied.

Several evidences have demonstrated the usefulness of attenuated total reflection/Fourier transform infrared (ATR/FT-IR) spectroscopy in the non-destructive analysis of biological tissues and biomaterials, quantitative determination of polymer coating, and reaction kinetics and structure development in polymer processing [11–18]. We have previously explored a series of studies by using the reflectance or transmission microscopic FT-IR/DSC system to simultaneously investigate the polymorphic and glass transition temperature of drugs, polymers and liquid crystal, the lipid thermotropic transition and protein conversion in skin, and the kinetics of thermal-dependent condensation of polymer [19–26]. In this study, we report the first use of a

* Corresponding author at: Biopharmaceutics Laboratory, Department of Medical Research and Education, Veterans General Hospital—Taipei, Taipei, Taiwan, ROC. Fax: +886-2-2875-1562; E-mail: sylin@isc1.vghtpe.gov.tw

0032-3861/99/$ - see front matter
PII: S0032-3861(98)00512-6

newly developed thermal micro attenuated total reflection/ Fourier transform infrared (ATR/FT-IR) spectroscopic system with curve-fitting program to quantitatively investigate the molecular structure of PNIPAAM in water below and above their LCST.

2. Experimemtal

2.1. Polymerization

N-isopropylacrylamide (NIPAAM, Eastman Kodak Co., USA) was recrystallized from n-hexane. NIPAAM (3 g) was dissolved in 30 ml of deionized, distilled water containing 0.6 g of ammonium persulfate and bubbled with nitrogen to remove the dissolved oxygen. This solution was poured into 150 ml of paraffin oil containing 1% of pluronic L-61, which was previously purged with nitrogen. The agitation speed was 500 rpm in a three-necked reaction bottle, and nitrogen was continously supplied in the course of study. After the formation of aqueous droplets in the oil phase was confirmed, 3 ml of *N*, *N*, *N′*, *N′*-tetraethylmethylenediamine was added to the continuous phase to initiate redox polymerization, which was performed at room temperature for 3 h. After polymerization, the mixture was separated out by excess deionized water, washed several times with mixture of acetone and deionized water (1:1) to remove the monomer, and then centrifuged [27,28]. The resulting mass was dissolved in 200 ml of distilled water and dialyzed, then precipitated in a equal volume of methanol and vacuum-dried. The unfractionated polymer was redissolved in distilled water with 0.5% (w/v) for further use.

2.2. Thermal analysis

A differential scanning calorimeter (DSC-910, TA Instruments, USA) was used. The heating rate was 1°C/min, with an open pan system in an N_2 gas flow. The instrument was calibrated with indium. The unfractionated polymer solution was transferred to the sample cell with a syringe. Polymer-free distilled water was placed in the reference cell [9].

2.3. Cloud point measurement

The cloud point of the unfractionated polymer solution was measured using spectrophotometer (UV-560, Jasco, Japan) with a water-jacketed cell holder coupled with a temperature-controlled circulating bath. The transmittance of sample solution at different temperatures was recorded at 600 nm. The accuracy of the temperature regulation was within $\pm$ 0.5°C [29].

2.4. Thermal micro ATR/FT-IR spectroscopic study

The DSC microscopy cell (FP 82, Mettler, Switzerland) was placed on the stage of the FT-IR microscopic spectrometer (Micro FTIR-200, Jasco, Japan) equipped with MCT detector with a resolution of 4 cm^{-1}. A copper vessel (1 ml in volume, 20 mm in diameter), filled with 1 ml of the unfractionated polymer solution, was settled onto this DSC microscopy cell. The ATR attachment (ATR-LG, prism: Ge) was descended into the vessel and just attached to the sample solution. The background absorbance of water was previously determined to act as a reference, which can be automatically subtracted from the absorbance of sample. The temperature of the DSC microscopy cell was monitored by a central processor (FT80HT, Mettler, Switzerland) from 25 to 60°C, but the actual temperature of the sample solution was monitored by a thermocouple previously inserted into vessel. A thermal gradient across the vessel could result in a difference of 1°–2°C between the recorded DSC cell temperature and the actual temperature of the solution. The heating rate was controlled at 1°C/min. The DSC thermograms and IR spectra could be simultaneously recorded. The component of each amides I and II in IR spectrum at the different temperatures was estimated quantitatively by curve-fitting program [30,31]. The proportion of a component was computed to be the fractional area of the corresponding peak, divided by the sum of the areas of peaks.

3. Results and discussion

The cloud point was determined by spectrophotometric detection of the changes in the turbidity of sample solution heated at different temperatures. We have found that the turbidity of PNIPAAM aqueous solution changed gradually with the increase of temperature but increased deeply after 33°C, which may be related to LCST, and the onset of turbidity was not so sharp. Moreover, a clear endothermic peak at 34.5°C was obviously observed in the DSC thermogram in which the onset temperature was also found at 33°C. This suggests that the temperature at 33°C may correspond to the phase transition and be defined as the LCST of PNIPAAM used.

A three-dimensional plot of the micro ATR/FT-IR spectra of PNIPAAM in water as a function of temperature is shown in Fig. 1. The temperature-dependent alterations in peak intensity of IR spectra were found. Apparently, the peak intensity of PNIPAAM increased dramatically after 33°C. Since the amide chains are included in the PNIPAAM structure, they have amides I and II bands in IR spectrum like polypeptide. The principal contribution to the amide I band is the carbonyl stretching vibration, but the amide II is mainly due to N–H bending vibration [32]. Both vibrations can be influenced by hydrogen bonding. PNIPAAM, like nylon, may have its amides I and II regions assumed to be composed of three distinct bands [30]: intramolecular hydrogen bonded C=O band at 1631 cm^{-1}, intermolecular hydrogen bonded C=O band at 1620 cm^{-1} and free form of non-hydrogen bonded C=O band at 1643 cm^{-1} for amide I;

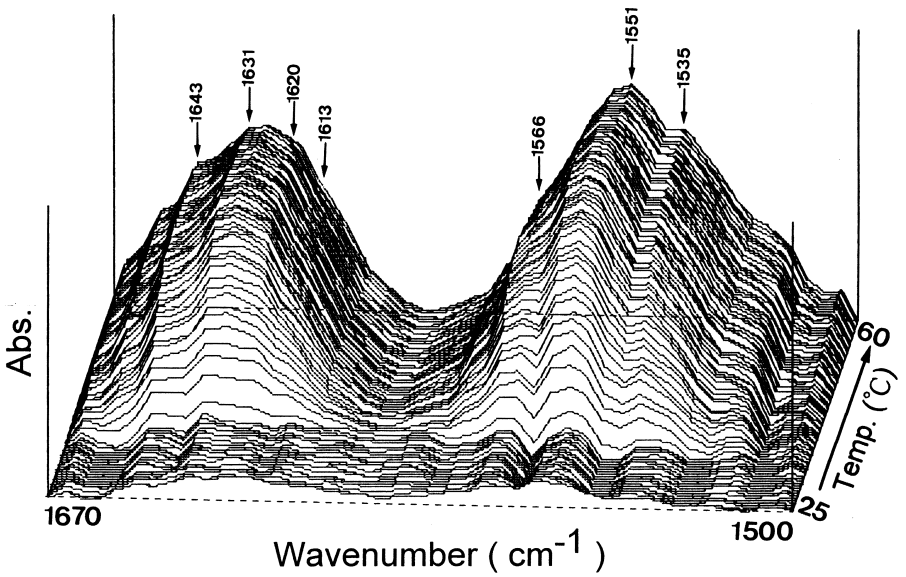

Fig. 1. Three-dimensional plot of ATR/FT-IR spectra of PNIPAAM as a function of temperature.

intramolecular hydrogen bonded N–H band at 1551 cm^{-1}, intermolecular hydrogen bonded N–H band at 1565 cm^{-1} and free form of non-hydrogen bonded N–H band at 1535 cm^{-1} for amide II [33,34]. The representative best curve-fitted original amides I and II IR spectra of this PNIPAAM in water at 25 and 55°C are shown in Fig. 2. Each spectrum is found to resolve into three components best-fitted by a least-squares iterative procedure.

The best curve-fitted results for the amides I and II of PNIPAAM in water throughout the temperature range

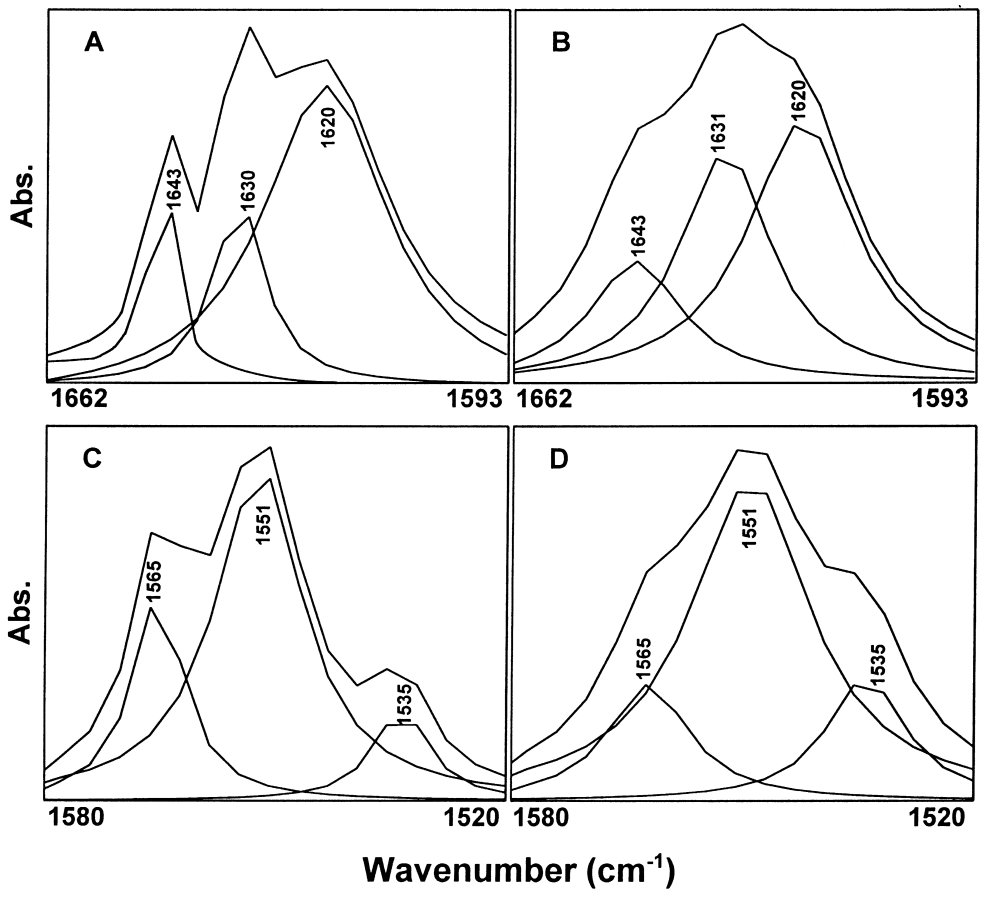

Fig. 2. The representative best curve-fitted original amides I and II IR spectra of PNIPAAM in water at 25°C (A, C) and 55°C (B, D).

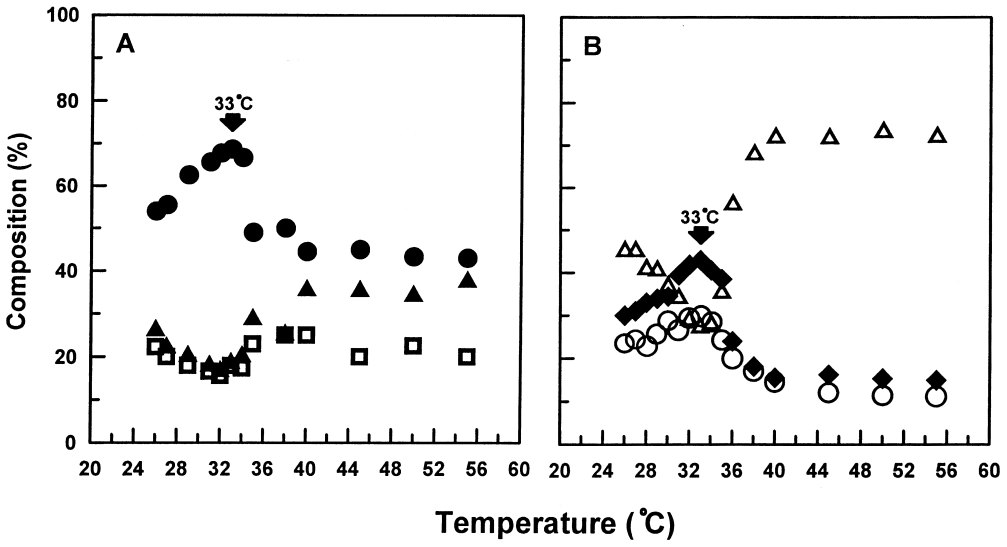

Fig. 3. The best curve-fitted components for the amides I and II of PNIPAAM in water throughout the temperature range 25°–60°C. Key: (□) 1643 cm^{-1}; (▲) 1631 cm^{-1}; (●) 1620 cm^{-1}; (♦) 1565 cm^{-1}; (△) 1551 cm^{-1}; (○) 1535 cm^{-1}.

25°–60°C are given in Fig. 3. In the carbonyl-related amide I region (Fig. 3A), below 33°C the composition of the band at 1620 cm^{-1} for intermolecular hydrogen bonding was the major proportion (about 50%–70% of total molecular interaction), and tended to increase with temperature. This reveals that below the LCST the intermolecular hydrogen bonding between carbonyl group of PNIPAAM and water played a predominant role in the molecular structure of PNIPAAM in water. The compositions of the intramolecular hydrogen bonded C=O group and the free form of non-hydrogen bonded C=O group were similar and exhibited the minor domain. Below the LCST, the enhancement of the intermolecular hydrogen bonded composition with temperature might be attributed to the thermodynamic activity of the temperature effect. However, once the temperature went beyond the LCST, the composition of the intermolecular hydrogen bonding decreased markedly from 70% to 45%. Moreover, the intramolecular hydrogen bonded composition was enhanced from 20% to 40% and was close to that of the intermolecular hydrogen bonded composition. Thus, above the LCST both the intra- and intermolecular hydrogen bondings played a dominant role in the molecular structure of PNIPAAM in water. In NH-related amide II region (Fig. 3B), a similar result was also found. Above the LCST, the intramolecular hydrogen bonded composition increased dramatically from 20%–40% to 70% with the increase of temperature and the intermolecular hydrogen bonded and non-hydrogen bonded compositions also decreased significantly, suggesting that the intramolecular hydrogen bonding was the major domain for PNIPAAM molecule in water. The results strongly indicate that below the LCST, the PNIPAAM molecule in water exhibited predominantly intermolecular hydrogen bonding between PNIPAAM molecule and water, but above LCST the intermolecular hydrogen bonding model transformed to the intramolecular hydrogen bonded conformation.

The hydrophobic *N*-isopropyl groups affecting the PNIPAAM conformation in water were also investigated. Fig. 4 shows the stretching and bending vibrational IR spectra of isopropyl groups of PNIPAAM at the different temperatures. The range between 3000 and 2835 cm^{-1} belongs to the C–H stretching vibration, in which the peaks at 2974 and 2876 cm^{-1} were assigned to asymmetric and symmetric vibrations of methyl group, and the peak at 2932 cm^{-1} was due to the asymmetric vibration of methylene group. Furthermore, the peak ranging from 1400–1355 cm^{-1} corresponded to the bending vibrations of isopropyl groups [35]. Since the methylene group was located on the backbone of PNIPAAM structure and was not influenced by the temperature, the peak area of 2932 cm^{-1} can act as an internal control. Each peak area for methyl and isopropyl groups of PNIPAAM at different temperatures divided by the peak area of 2932 cm^{-1} was computed, and the results are indicated in Fig. 5. Apparently, above the LCST all the peak area ratios, 2974 cm^{-1}/2932 cm^{-1}, 2876 cm^{-1}/2932 cm^{-1} and 1400–1355 cm^{-1}/2932 cm^{-1} increased dramatically with the increase of temperature, respectively. The hydrophobic behavior of methyl group in PNIPAAM molecule enhanced 1.5 times when the temperature was above the LCST. Below the LCST these peak area ratios reduced with the increase of temperature. This suggests again that, until minor behavior below the LCST, the hydrophobic *N*-isopropyl groups in the PNIPAAM molecule in water exhibited a considerably hydrophobic function above the LCST to induce the aggregation of PNIPAAM polymer. Thus, when the temperature was below the LCST, the hydrophobic isopropyl groups in PNIPAAM molecule should be embedded into the central part of molecule and the hydrophilic C=O and NH groups in molecule were dominantly exposed to the outer layer to contact with water to achieve higher composition of intermolecular hydrogen bonding. When the temperature went beyond the LCST, the intermolecular

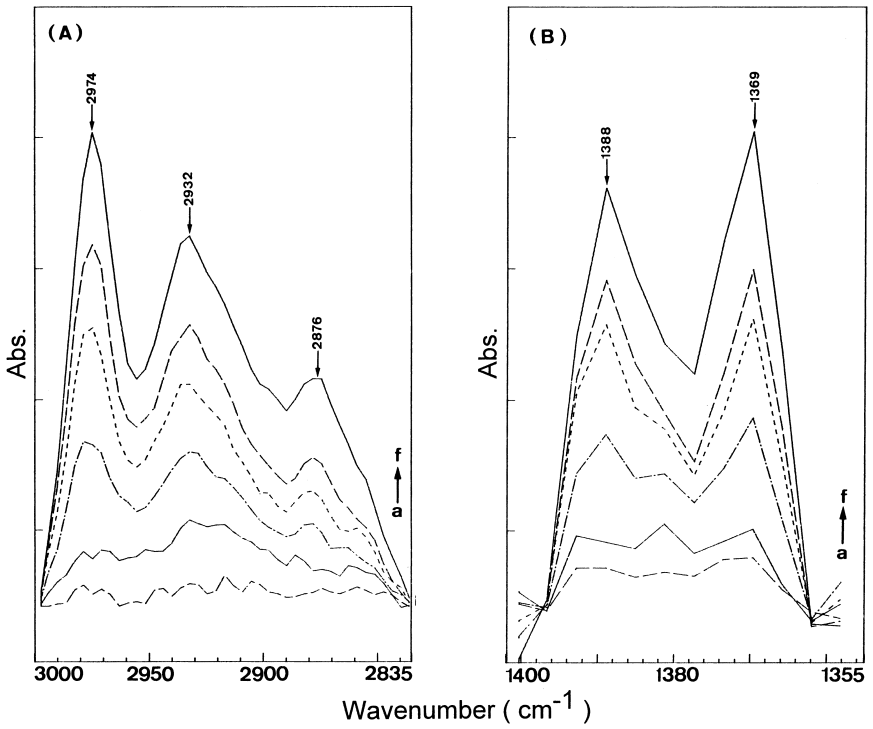

Fig. 4. The stretching (A) and bending (B) vibrational IR spectra of isopropyl groups in PNIPAAM at the different temperatures. Key: (a) 25°C; (b) 32°C; (c) 33°C; (d) 35°C; (e) 37°C; (f) 55°C.

hydrogen bonding model of PNIPAAM molecule was reversibly transformed to the intramolecular hydrogen bonded conformation. At the same time, the hydrophobic isopropyl groups were exposed to outer layer to form hydrophobic effect. The aggregation phenomenon of PNIPAAM might be attributable to both the intramolecular interactions and the hydrophobic interactions.

4. Conclusions

A newly developed thermal micro ATR/FT-IR spectroscopic system has been successfully and quantitatively applied to investigate the LCST and the molecular structure of PNIPAAM in water. Below the LCST, the molecular structure of PNIPAAM in water exhibited a predominantly

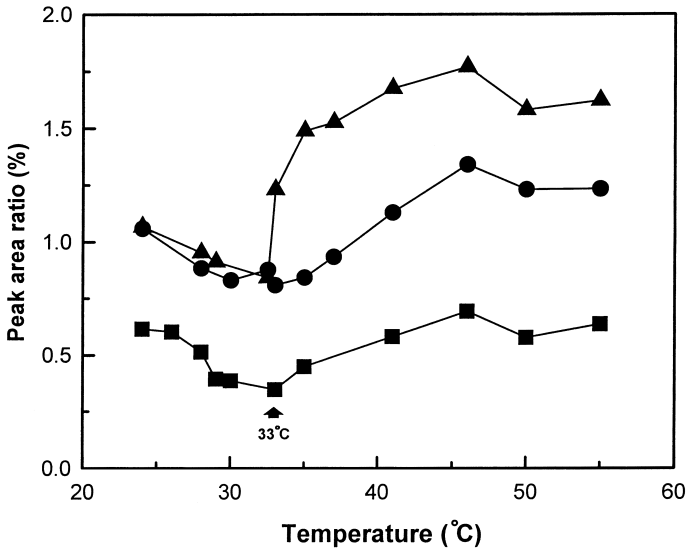

Fig. 5. Plot of the peak area ratios as a function of temperature for PNIPAAM in water. Key: (▲) 2974 cm^{-1}/2932 cm^{-1}; (■) 2876 cm^{-1}/2932 cm^{-1}; (●) 1400–1355 cm^{-1}/2932 cm^{-1}.

intermolecular hydrogen bonding (about 50%–70% of total molecular interaction estimated from amide I band) between PNIPAAM and water. However, above the LCST the intramolecular hydrogen bonded conformation was about 70% in total molecular interaction (estimated from amide II band). Moreover, the hydrophobic interaction of methyl group in PNIPAAM molecule enhanced 1.5 times when the temperature was above the LCST. The results quantitatively represent that the intermolecular interactions might occur between PNIPAAM and water when the temperature was below the LCST. Beyond that temperature, however, PNIPAAM was coagulated due to the intramolecular interactions mainly of PNIPAAM molecules and the hydrophobic interactions. Thermal micro ATR/FT-IR spectroscopic system is useful to quantitatively detect the molecular interaction of PNIPAAM in water. Further examination of the molecular interaction of crosslinked PNIPAAM gel in water below and above the LCST will be done in a forthcoming study.

References

[1] Hoffman AS. J Control Rel 1987;6:297.
[2] Okano T, Bae YH, Jacobs H, Kim SW. J Control Rel 1990;11:255.
[3] Yoshida R, Kaneko Y, Sakai K, Okano T, Sakurai Y, Bae YH, Kim SW. J Control Rel 1994;32:97.
[4] Nguyen AL, Luong JHT. Enzyme Microb Technol 1990;12:663.
[5] Park TG, Hoffman AS. Appl Biochem Biotechnol 1988;19:1.
[6] Takezawa T, Mori Y, Yoshizato K. Biotechnology 1990;8:854.
[7] Schild HG. Prog Polym Sci 1992;17:163.
[8] Yoshida R, Uchida K, Kaneko Y, Sakai K, Kikuchi A, Sakurai Y, Okano T. Nature 1995;374:240.
[9] Otake K, Inomata H, Konno M, Saito S. Macromolecules 1990;23:283.
[10] Inomata H, Goto S, Saito S. Macromolecules 1990;23:4887.
[11] Ozaki Y, Kaneuchi F, Iwamoto T, Yoshimura M, Iriyama K. Appl Spectrosc 1989;43:138.
[12] Singh BR, Fuller MP. Appl Spectrosc 1991;45:1017.
[13] Baraga JJ, Feld MS, Rava RP. Appl Spectrosc 1991;45:709.
[14] Sutherland K, Mahoney JR, Coury AJ, Eaton J. J Clin Invest 1993;92:2360.
[15] Magnani A, Busi E, Barbucci R. J Mater Sci: Mater Med 1994;5:839.
[16] Dupuy N, Ruckebush C, Duponchel L, Beurdeley-Sausou P, Amram B, Huvenne JP, Legrand P. Anal Chim Acta 1996;335:79.
[17] Church JS, Evans DI. J Appl Polym Sci 1995;57:1585.
[18] Bras W, Derbyshire DE, Bogg D, Cooke J, Elwell MJ, Komanschek BU, Naylor S, Ryan AJ. Science 1995;267:996.
[19] Lin SY. J Pharmac Sci 1992;81:572.
[20] Lin SY, Liang RC, Lin TC. J Chin Chem Soc—Taipei 1994;41:425.
[21] Lin SY, Liao CM, Liang RC. Polym J 1995;27:201.
[22] Lin SY, Liao CM, Hsiue GH. Polym Degrad Stabil 1995;47:299.
[23] Lin SY, Lin YY, Chen KS. Drug Deliv 1995;2:123.
[24] Lin YY, Chen KS, Lin SY. J Chin Chem Soc—Taipei 1995;42:865.
[25] Lin SY, Liao CM, Hsiue GH. Polymer 1996;37:269.
[26] Lin SY, Duan KJ, Lin TC. Spectrochim Acta A 1996;52:1671.
[27] Park TG, Hoffman AS. Biotechnol Prog 1994;10:82.
[28] Schild HG, Tirrell DA. J Phys Chem 1990;94:4352.
[29] Fujishige S, Kubota K, Ando L. J Phys Chem 1989;93:3311.
[30] Skrovanek DJ, Painter PC, Coleman MM. Macromolecules 1986;19:699.
[31] Musto P, Karasz FE, MacKnight WJ. Macromolecules 1991;24:4762.
[32] Harris PI, Chapman D. Trends Biol Sci 1992;17:328.
[33] Pimentel GC, McClellan AL. In The hydrogen bond. San Francisco, CA: WH Freeman, 1960:87.
[34] Pretsch E, Seibl J, Simon W, editors. Tables of spectral data for structure determination of organic compounds, 2nd ed. Berlin: Springer, 1989:150.
[35] Pavia DL, Lampman GM, Kriz GS, editors. Introduction to spectroscopy: a guide for students of organic chemistry. Philadelphia, PA: WB Saunders, 1979:27–37.